

# Nonlinear Feed Effect in Machining Chatter Analysis

**Robert G. Landers**

Department of Mechanical and Aerospace  
Engineering,  
University of Missouri-Rolla,  
Rolla, MO 65409-0050  
e-mail: landersr@umr.edu

**A. Galip Ulsoy**

Department of Mechanical Engineering,  
University of Michigan,  
Ann Arbor, MI 48109-2125  
e-mail: ulsoy@umich.edu

*Regenerative chatter is a major limitation to the productivity and quality of machining operations due to the excessive rate of tool wear and scrap parts which are produced. Machining chatter analysis techniques examine the stability of the closed-loop model (force process and machine tool-part structure) of the machining operation to determine the stable process parameter space. Almost all chatter analysis techniques assume a linear force process and develop stability lobe diagrams (i.e., plots of the stable and unstable regions in the process parameter space) for a specific feed. It is well known that machining force processes inherently contain a nonlinear relationship between the force and the feed, which is typically described by a power law. In this paper, the linear chatter analysis technique developed by Budak and Altintas is extended to account for the force-feed nonlinearity. The analysis provides insight into the effect feed has on chatter in machining operations. Also, by directly including the force-feed nonlinearity in the chatter analysis, the need to calibrate the force process model at different feeds is alleviated. The analysis is developed for turning and face milling operations and is validated via time domain simulations for both operations and by experiments for a face milling operation. The analyses show excellent agreement with both the time domain simulations and the experiments. Further, several end milling experiments were conducted that illustrate the nonlinear effect feed has on chatter in machining operations.*

[DOI: 10.1115/1.2783276]

## Introduction

Regenerative chatter occurs in machining operations due to the closed-loop interaction between the machine tool-part structural displacements and the force process. Each tooth pass leaves a modulated surface on the part due to the displacements of the machine tool and part structures, causing a variation in the chip thickness during the next tooth pass. For certain combinations of process parameters (i.e., feed, depth-of-cut, and speed), large chip thickness variations, and hence force and displacement variations, occur and chatter is present. Chatter can result in machine tool damage, excessive rate of tool wear, and scrap parts. Machine tool operators often select conservative process parameters to avoid chatter, thus, decreasing productivity.

Since extensive experimentation is typically not cost effective, analysis techniques are used to generate the so-called stability lobe diagrams (SLDs): plots of the stable and unstable regions in the process parameter space. SLDs may be used for process planning of chatter-free machining operations and for machine tool design. All regenerative chatter analysis techniques begin with a model of the machining force process and a model of the machine tool-part structure. These two models are combined to form a closed-loop dynamic model of the machining operation. One of the earliest analysis techniques was developed by Merritt [1] who generated specialized plots from the harmonic solutions of the system's characteristic equation to determine system stability and construct SLDs. Many researchers have used Nyquist techniques to generate SLDs [2,3]. A set of process parameters (e.g., depth-of-cut and spindle speed) are selected and the characteristic equation is formed. The Nyquist criterion is applied to determine if the process parameters are stable. The critical process parameter (e.g., depth-of-cut) is adjusted and the procedure is repeated until the marginally stable value is determined. Olgac and Hosek [4] used a root locus analysis of time delayed systems to explore regenerative chatter. Another chatter analysis technique used to generate

SLDs for end milling operations was proposed by Budak and Altintas [5]. Assuming a single chatter frequency, analytical expressions for the limiting depth-of-cut and spindle speed are obtained. This approach was applied to turning operations in Landers [6] and face milling operations in Jensen and Shin [7,8] and Landers [6], and will be extended in this paper to explore the nonlinear force-feed effect in these operations.

Time domain simulation (TDS) is another technique that may be used to generate SLDs [9–11]. The closed-loop dynamic model of the machining operation is simulated for a particular set of process parameters. Steady-state machine tool and part displacements and machining force signals are examined to determine system stability. The critical process parameter (e.g., depth-of-cut) is adjusted until marginal stability is encountered. The strength of TDS is that one may incorporate all major aspects of the machining operation, including nonlinear characteristics, into the chatter analysis. However, the inherent drawback to using TDS is the computational burden imposed by having to run a multitude of simulations.

Two recent works have examined the effect of the force-feed nonlinear relationship on machining chatter. Zhang and Ni [12] developed a criterion based upon the phase difference between the current and previous tooth passes to determine the presence of chatter. They approximately included the force-feed nonlinearity by expanding the nonlinear term with a Taylor series expansion. Endres [13] used TDS and an extension of a linear energy-based analysis [14] to investigate stability limits for a one-dimensional orthogonal machining operation. He considered the nonlinear force-feed effect by linearizing the relationship about one nominal feed and concluded that the nonlinearity does not affect the stability limit but does affect the magnitude of the chatter vibrations. However, both research studies [12,13] did not consider the effect of the nominal feed on the stability limit. This paper extends the chatter analyses for turning and milling in Landers [6] to include the effect of force-feed nonlinearities. The analyses and results provide insight into the effect feed has on chatter in machining operations. Simulation and experimental results demonstrate the significant effect the force-feed nonlinearity has on chatter and validates the developed chatter analyses.

Contributed by the Manufacturing Engineering Division of ASME for publication in the JOURNAL OF MANUFACTURING SCIENCE AND ENGINEERING. Manuscript received January 22, 2007; final manuscript received July 31, 2007; published online February 15, 2008. Review conducted by William J. Endres.

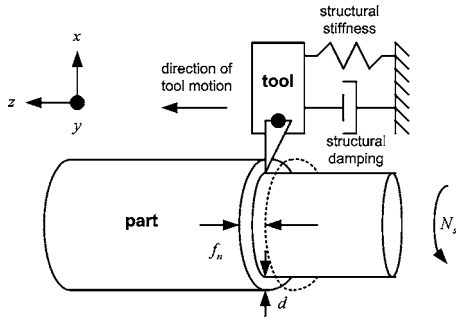


**Fig. 1 Turning operation schematic (dashed line is tool trajectory during previous spindle rotation)**

## Effect of Force-Feed Nonlinearity in Turning Operations

In this section the effect of the nonlinear force-feed relationship on chatter in turning operations is investigated. A linearization analysis is utilized to explore this effect and the analysis results are compared to time domain simulations. A schematic of a turning operation is shown in Fig. 1. The part structure is assumed to be perfectly rigid, while the cutting tool structure vibrates in the  $z$  direction only. The longitudinal machining force is modeled as [6]

$$F(t) = Pdf(t) = Kdf^\alpha(t) \quad (1)$$

where  $P$  is the longitudinal pressure;  $d$  is the depth-of-cut;  $f$  is the feed; and  $K$  and  $\alpha$  are empirically determined model constants. The depth-of-cut and nose radius also have nonlinear effects on the longitudinal machining force. However, they are not included in this study so that the nonlinear feed effect can be highlighted. Further study would be required to include these nonlinear effects. The depth-of-cut is assumed to be constant; however, the feed, and hence the machining force, is time varying due to structural displacements. The longitudinal pressure is influenced by many factors such as tool geometry, cutting tool and part materials, cutting fluid, etc., which are constant during the machining operation. It is also well known that the machining pressure is a function of the instantaneous feed. This relationship is typically represented by a power law as in Eq. (1). When  $\alpha \neq 1$ , the force-feed relationship is nonlinear. It is assumed here that the machining force does not explicitly depend upon the cutting speed and the machining force is linearly related to the depth-of-cut. The nominal feed is the distance the cutting tool advances relative to the part in the longitudinal direction of each spindle revolution due to the servomechanism that provides the cutting tool's longitudinal motion. The cutting tool, however, vibrates about its nominal position leaving an undulated surface on the part, which modulates the feed. The instantaneous feed is

$$f(t) = f_n + z(t) - z(t-T) \quad (2)$$

where  $f_n$  is the nominal (i.e., static) feed and  $T$  is the spindle revolution period. The structural displacement  $z(t)$ , known as the inner modulation, is the cutting tool structural displacement at the current time. The structural displacement  $z(t-T)$ , known as the outer modulation, is the cutting tool structural displacement when the part was at the current spatial location during the previous spindle rotation. Inserting Eq. (2) into Eq. (1)

$$F(t) = Kd[f_n + z(t) - z(t-T)]^\alpha \quad (3)$$

Linearizing Eq. (3) about the nominal feed and noting that the structural displacement is constant at the nominal conditions

$$F(t) = Kdf_n^\alpha + \alpha Kdf_n^{\alpha-1}[f(t) - f_n] = F_n + \alpha Kdf_n^{\alpha-1}[z(t) - z(t-T)] \quad (4)$$

where  $F_n = Kdf_n^\alpha$  is the nominal force. Eq. (4) can be rewritten as

$$\Delta F(t) = \alpha Kdf_n^{\alpha-1} \Delta z(t) \quad (5)$$

where  $\Delta F(t) = F(t) - F_n$  and  $\Delta z(t) = z(t) - z(t-T)$ . The structural displacements are related to the machining force by

$$z(s) = -g(s)F(s) \quad (6)$$

Noting that  $F(t) - F(t-T) = \Delta F(t) - \Delta F(t-T)$ , the structural displacements are related to the machining forces by

$$\Delta z(s) = -(1 - e^{-sT})g(s)\Delta F(s) \quad (7)$$

Taking the Laplace transform of Eq. (5) with zero initial conditions, substituting the resulting equation into Eq. (7), and rearranging

$$\Delta F(s)\{1 + \alpha Kdf_n^{\alpha-1}d[1 - e^{-sT}]g(s)\} = 0 \quad (8)$$

Equation (8) is now solved, based on the method presented by Budak and Altintas [5], to determine the conditions for marginal stability. Assuming the steady-state solution is undamped and oscillates at a single chatter frequency  $\omega_c$ , Eq. (8) becomes

$$\Delta F(j\omega_c)\{1 + \alpha Kdf_n^{\alpha-1}d[1 - e^{-j\omega_c T}]g(j\omega_c)\} = 0 \quad (9)$$

where  $j$  is the imaginary number. For nontrivial solutions of Eq. (9)

$$1 + \alpha Kdf_n^{\alpha-1}d[1 - e^{-j\omega_c T}]g(j\omega_c) = 0 \quad (10)$$

The parameter  $\Lambda$  is defined as

$$\Lambda = \alpha Kdf_n^{\alpha-1}d[1 - e^{-j\omega_c T}] = \Lambda_R + j\Lambda_I \quad (11)$$

Using the Euler identity and solving Eq. (11) for the limiting depth-of-cut

$$d = \left( \frac{1}{2\alpha Kdf_n^{\alpha-1}} \right) \left\{ \frac{\Lambda_R[1 - \cos(\omega_c T)] + \Lambda_I \sin(\omega_c T)}{1 - \cos(\omega_c T)} \right. \\ \left. - j \frac{\Lambda_R \sin(\omega_c T) - \Lambda_I [1 - \cos(\omega_c T)]}{1 - \cos(\omega_c T)} \right\} \quad (12)$$

Since the limiting depth-of-cut is a real number

$$\Lambda_R \sin(\omega_c T) - \Lambda_I [1 - \cos(\omega_c T)] = 0 \quad (13)$$

and Eq. (12) can be rewritten as

$$d = \frac{\Lambda_R}{2\alpha Kdf_n^{\alpha-1}}(1 + \kappa^2) \quad (14)$$

where the parameter  $\kappa$  is

$$\kappa = \frac{\Lambda_I}{\Lambda_R} = \frac{\sin(\omega_c T)}{1 - \cos(\omega_c T)} \quad (15)$$

It can be seen from Eq. (14) that the nonlinear feed effect directly changes the limiting depth-of-cut by a factor of  $1/\alpha f_n^{\alpha-1}$ . Note that when  $\alpha=1$  this factor equals 1. Therefore, depending on the value of the parameter  $\alpha$  and the range of feeds, increasing the feed may either increase or decrease the limiting depth-of-cut. The nontrivial solution to Eq. (15) is

$$\cos(\omega_c T) = \frac{\kappa^2 - 1}{\kappa^2 + 1} \quad (16)$$

Solving for the quantity  $\omega_c T$

$$\omega_c T = \varepsilon + 2l\pi \quad l = 0, 1, 2, \dots \quad (17)$$

where

$$\varepsilon = \cos^{-1} \left( \frac{\kappa^2 - 1}{\kappa^2 + 1} \right) \quad (18)$$

The parameter  $\varepsilon$  is the fraction of the vibration cycles during a spindle rotation. The angle of  $\Lambda$  in the complex plane is

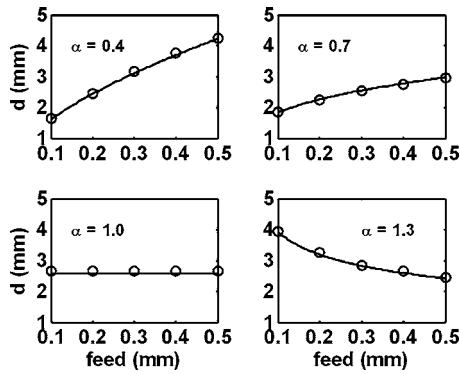


**Fig. 2** Feed-depth stability lobe diagrams for the turning simulation study with  $N_s=7391$  rpm. Solid lines are analyses and circles are time domain simulations. Error bars are not shown as they are smaller than the marker size.

$$\varphi = \tan^{-1}\left(\frac{\Lambda_I}{\Lambda_R}\right) = \tan^{-1}(\kappa) \quad (19)$$

Substituting  $\kappa = \tan(\varphi)$  into Eq. (16) yields

$$\cos(\omega_c T) = -\cos(2\varphi) \quad (20)$$

A solution to Eq. (20) is

$$\omega_c T = \pi - 2\varphi + 2l\pi \quad l = 0, 1, 2, \dots \quad (21)$$

Comparing Eqs. (17) and (21), the fraction of vibration cycles is  $\varepsilon = \pi - 2\varphi$ . The spindle speed is

$$N_s = \frac{60}{T} = \frac{60\omega_c}{\varepsilon + 2l\pi} \quad l = 0, 1, 2, \dots \quad (22)$$

### Turning Simulation Studies

Simulation studies are conducted in this section to investigate the effect that the nonlinear force-feed relationship has on chatter in turning operations. The longitudinal machining force is given by Eq. (1) where  $K=1.2$ . Four values of  $\alpha$  will be investigated: 0.4, 0.7, 1.0, and 1.3. The structural displacements are given by Eq. (6) where

$$g(s) = \frac{\omega_n^2 k^{-1}}{s^2 + 2\zeta\omega_n s + \omega_n^2} \quad (23)$$

$k=12$  kN/mm,  $\zeta=0.1$ , and  $\omega_n=600$  Hz. For each simulation study the chatter frequency is  $\omega_c=700$  Hz and the fifth stability lobe is investigated. These parameters correspond to a spindle speed of  $N_s=7391$  rpm. The analytical results are compared to TDSs where the machining force process and structural displacements are simulated simultaneously. The simulations utilize a fourth-order Runge–Kutta integration routine and 2880 samples/rev yielding a sample period of  $2.819 \cdot 10^{-6}$  s. To determine each TDS point, the closed-loop machining system is simulated with a fixed set of process parameters for several revolutions and the longitudinal force signal is examined. The depth-of-cut is adjusted in increments of 0.1 mm until stable and unstable depths-of-cut are encountered at successive increments.

Simulation results are shown in Fig. 2. For each value of  $\alpha$ , the linearized analysis predicted the limiting depth-of-cut for marginal stability, as compared to the TDS results, very well, with a maximum percent error of 3.42%. For  $\alpha=1$ , the limiting depth-of-cut is constant for all feeds since, in this case, Eq. (12) reduces to  $d = \Lambda_R/2K(1 + \kappa^2)$ , which is independent of the feed. For  $\alpha=0.4$  and 0.7, the limiting depth-of-cut increases as the feed increases in a nonlinear manner with the slope asymptotically approaching zero as the feed approaches infinity. The change is more dramatic for smaller values of  $\alpha$ . For  $\alpha=1.3$ , the effect is opposite: the limiting

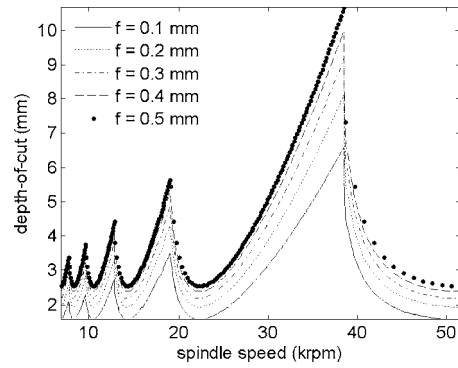


**Fig. 3** Stability lobe diagrams for the turning simulation study

depth-of-cut decreases as the feed increases, also in a nonlinear manner. Complete stability lobe diagrams are constructed for the first five lobes for feeds of 0.1 mm, 0.2 mm, 0.3 mm, 0.4 mm, and 0.5 mm and  $\alpha=0.7$ . The results are shown in Fig. 3. It can be seen that for all spindle speeds the limiting depth-of-cut increases as the feed increases.

### Effect of Force-Feed Nonlinearity in Face Milling Operations

In this section the effect that the force-feed nonlinearity has in face milling operations is investigated. A linearization analysis is utilized to explore this effect and the analysis results are compared to time domain simulations and experimental results for a face milling operation. The two major force components acting on a tooth during a face milling operation are the cutting and thrust forces (Fig. 4). The cutting and thrust forces, respectively, acting on the  $i$ th tooth are

$$F_{C_i} = P_{C_i} df_i = K_{C_i} df_i^{\alpha_{C_i}} \quad (24)$$

$$F_{T_i} = P_{T_i} df_i = K_{T_i} df_i^{\alpha_{T_i}} \quad (25)$$

where  $P_{C_i}$  and  $P_{T_i}$  are the cutting and thrust pressures, respectively, acting on the  $i$ th tooth;  $d$  is the depth-of-cut;  $f$  is the feed; and  $K_{C_i}$ ,  $\alpha_{C_i}$ ,  $K_{T_i}$ , and  $\alpha_{T_i}$  are empirically determined model constants.

Referring to Fig. 4, the feed of the  $i$ th tooth is

$$f_i(t) = f_i \cos[\theta_i(t)] + \Delta x(t) \cos[\theta_i(t)] + \Delta y(t) \sin[\theta_i(t)] \quad (26)$$

where

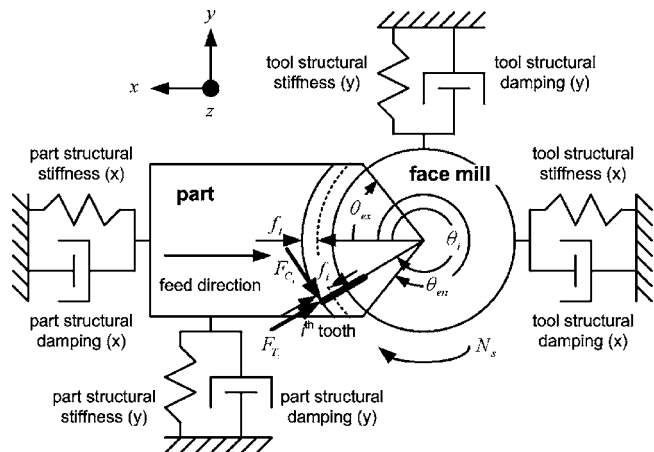


**Fig. 4** Face milling operation schematic (dashed line is previous tooth trajectory)

$$\Delta x(t) = [x_t(t) - x_t(t - T_i)] - [x_p(t) - x_p(t - T_i)] \quad (27)$$

$$\Delta y(t) = [y_t(t) - y_t(t - T_i)] - [y_p(t) - y_p(t - T_i)] \quad (28)$$

and  $T_i$  is the tooth passing period. The parameters  $\Delta x(t)$  and  $\Delta y(t)$  are the differences between the current and previous machine tool and part structural displacements in the  $x$  and  $y$  directions, respectively, and represent the modulation in feed due to machine tool and part structural displacements. The motion in the  $z$  direction is ignored since vertical milling machines, which are the types of machine tools used in the subsequent experiments, are much stiffer in this direction than in the  $x$  and  $y$  directions.

Inserting Eq. (26) into Eqs. (24) and (25), respectively

$$F_{C_i} = K_C d [f_i \cos[\theta_i(t)] + \Delta x(t) \cos[\theta_i(t)] + \Delta y(t) \sin[\theta_i(t)]]^{\alpha_C} \quad (29)$$

$$F_{T_i} = K_T d [f_i \cos[\theta_i(t)] + \Delta x(t) \cos[\theta_i(t)] + \Delta y(t) \sin[\theta_i(t)]]^{\alpha_T} \quad (30)$$

Linearizing Eqs. (29) and (30), respectively, about the nominal feed trajectory  $f_i \cos[\theta_i(t)]$

$$F_{C_i}(t) = K_C d [f_i \cos(\theta_i(t))]^{\alpha_C} + \alpha_C K_C d [f_i \cos(\theta_i(t))]^{\alpha_C - 1} [f_i(t) - f_i \cos(\theta_i(t))] \quad (31)$$

$$F_{T_i}(t) = K_T d [f_i \cos(\theta_i(t))]^{\alpha_T} + \alpha_T K_T d [f_i \cos(\theta_i(t))]^{\alpha_T - 1} [f_i(t) - f_i \cos(\theta_i(t))] \quad (32)$$

Equations (31) and (32), respectively, can be rewritten as

$$F_{C_i}(t) = F_{C_{n,i}}(t) + \alpha_C K_C d [f_i \cos(\theta_i(t))]^{\alpha_C - 1} [\Delta x \cos(\theta_i(t)) + \Delta y \sin(\theta_i(t))] \quad (33)$$

$$F_{T_i}(t) = F_{T_{n,i}}(t) + \alpha_T K_T d [f_i \cos(\theta_i(t))]^{\alpha_T - 1} [\Delta x \cos(\theta_i(t)) + \Delta y \sin(\theta_i(t))] \quad (34)$$

where  $F_{C_{n,i}}(t) = K_C d [f_i \cos(\theta_i(t))]^{\alpha_C}$  and  $F_{T_{n,i}}(t) = K_T d [f_i \cos(\theta_i(t))]^{\alpha_T}$  are the nominal cutting and thrust force trajectories, respectively. The total forces acting on the cutting tool in the  $x$  and  $y$  directions, respectively, are

$$F_x(t) = \sum_{i=1}^{N_i} [-F_{T_i} \cos(\psi_r) \cos(\theta_i(t)) + F_{C_i} \sin(\theta_i(t))] \sigma(\theta_i(t)) \quad (35)$$

$$F_y(t) = \sum_{i=1}^{N_i} [-F_{T_i} \cos(\psi_r) \sin(\theta_i(t)) - F_{C_i} \cos(\theta_i(t))] \sigma(\theta_i(t)) \quad (36)$$

where  $N_i$  is the number of teeth and

$$\sigma(\theta_i(t)) = \begin{cases} 1 & \text{if } \theta_{en} < \theta_i(t) < \theta_{ex} \\ 0 & \text{if } \theta_{en} \geq \theta_i(t) \geq \theta_{ex} \end{cases} \quad (37)$$

The function  $\sigma(\theta_i(t))$  determines if the  $i$ th tooth is in contact with the part at time  $t$ . The summation from  $i=1$  to  $N_i$  represents the contribution of each tooth to this modulation.

Substituting Eqs. (33) and (34) into Eqs. (35) and (36), respectively, the resulting dynamic force process is

$$\begin{bmatrix} \Delta F_x(t) \\ \Delta F_y(t) \end{bmatrix} = dA(t) \begin{bmatrix} \Delta x(t) \\ \Delta y(t) \end{bmatrix} = d \begin{bmatrix} a_{11}(t) & a_{12}(t) \\ a_{21}(t) & a_{22}(t) \end{bmatrix} \begin{bmatrix} \Delta x(t) \\ \Delta y(t) \end{bmatrix} \quad (38)$$

where

$$\Delta F_x(t) = F_x(t) - \sum_{i=1}^{N_i} [-F_{T_{n,i}}(t) \cos(\psi_r) \cos(\theta_i(t)) + F_{C_{n,i}}(t) \sin(\theta_i(t))] \sigma(\theta_i(t)) \quad (39)$$

$$\Delta F_y(t) = F_y(t) - \sum_{i=1}^{N_i} [-F_{T_{n,i}}(t) \cos(\psi_r) \sin(\theta_i(t)) - F_{C_{n,i}}(t) \cos(\theta_i(t))] \sigma(\theta_i(t)) \quad (40)$$

$$a_{11}(t) = \sum_{i=1}^{N_i} [-\eta_T \cos^{\alpha_T + 1}(\theta_i(t)) + \eta_C \sin(\theta_i(t)) \cos^{\alpha_C}(\theta_i(t))] \sigma(\theta_i(t)) \quad (41)$$

$$a_{12}(t) = \sum_{i=1}^{N_i} [-\eta_T \sin(\theta_i(t)) \cos^{\alpha_T}(\theta_i(t)) + \eta_C \sin^2(\theta_i(t)) \cos^{\alpha_C - 1}(\theta_i(t))] \sigma(\theta_i(t)) \quad (42)$$

$$a_{21}(t) = \sum_{i=1}^{N_i} [-\eta_T \sin(\theta_i(t)) \cos^{\alpha_T}(\theta_i(t)) - \eta_C \cos^{\alpha_C + 1}(\theta_i(t))] \sigma(\theta_i(t)) \quad (43)$$

$$a_{22}(t) = \sum_{i=1}^{N_i} [-\eta_T \sin^2(\theta_i(t)) \cos^{\alpha_T - 1}(\theta_i(t)) - \eta_C \sin(\theta_i(t)) \cos^{\alpha_C}(\theta_i(t))] \sigma(\theta_i(t)) \quad (44)$$

$$\eta_C = \alpha_C K_C d f_i^{\alpha_C - 1} \quad (45)$$

$$\eta_T = \alpha_T K_T d \cos(\psi_r) f_i^{\alpha_T - 1} \quad (46)$$

The coefficients in the matrix  $A$  modulate the instantaneous feed as the tool angular displacement changes. Note the matrix  $A$  is time varying and periodic with a known period; namely, the tooth passing period. For chatter analysis, this matrix is expanded in a Fourier series [3,5]. The zeroth Fourier approximation of the force process matrix  $A$  is

$$A^0 = \frac{N_i}{2\pi} \begin{bmatrix} a_{11}^0 & a_{12}^0 \\ a_{21}^0 & a_{22}^0 \end{bmatrix} \quad (47)$$

where

$$a_{11}^0 = -\eta_T \int_{\theta_{en}}^{\theta_{ex}} [\cos^{\alpha_T + 1}(\theta)] d\theta + \eta_C \int_{\theta_{en}}^{\theta_{ex}} [\sin(\theta) \cos^{\alpha_C}(\theta)] d\theta \quad (48)$$

$$a_{12}^0 = -\eta_T \int_{\theta_{en}}^{\theta_{ex}} [\sin(\theta) \cos^{\alpha_T}(\theta)] d\theta + \eta_C \int_{\theta_{en}}^{\theta_{ex}} [\sin^2(\theta) \cos^{\alpha_C - 1}(\theta)] d\theta \quad (49)$$

$$a_{21}^0 = -\eta_T \int_{\theta_{en}}^{\theta_{ex}} [\sin(\theta) \cos^{\alpha_T}(\theta)] d\theta - \eta_C \int_{\theta_{en}}^{\theta_{ex}} [\cos^{\alpha_C + 1}(\theta)] d\theta \quad (50)$$

$$a_{22}^0 = -\eta_T \int_{\theta_{en}}^{\theta_{ex}} [\sin^2(\theta) \cos^{\alpha_T - 1}(\theta)] d\theta - \eta_C \int_{\theta_{en}}^{\theta_{ex}} [\sin(\theta) \cos^{\alpha_C}(\theta)] d\theta \quad (51)$$

The integrals in Eqs. (48)–(51) must be evaluated numerically. Note that for fixed values of  $\theta_{en}$ ,  $\theta_{ex}$ ,  $\alpha_C$ , and  $\alpha_T$ , these integrals

are constant and can be evaluated once before conducting the chatter analysis. The linear, time-invariant force process model is

$$\begin{bmatrix} \Delta F_x(t) \\ \Delta F_y(t) \end{bmatrix} = dA^0 \begin{bmatrix} \Delta x(t) \\ \Delta y(t) \end{bmatrix} \quad (52)$$

The machine tool structure (i.e., face mill, spindle unit, etc.) and the part structure (i.e., part, fixture, etc.) are modeled, respectively, by

$$\begin{bmatrix} x_t(s) \\ y_t(s) \end{bmatrix} = G_t(s) \begin{bmatrix} F_x(s) \\ F_y(s) \end{bmatrix} = \begin{bmatrix} G_{t11}(s) & G_{t12}(s) \\ G_{t21}(s) & G_{t22}(s) \end{bmatrix} \begin{bmatrix} F_x(s) \\ F_y(s) \end{bmatrix} \quad (53)$$

$$\begin{bmatrix} x_p(s) \\ y_p(s) \end{bmatrix} = -G_p(s) \begin{bmatrix} F_x(s) \\ F_y(s) \end{bmatrix} = -\begin{bmatrix} G_{p11}(s) & G_{p12}(s) \\ G_{p21}(s) & G_{p22}(s) \end{bmatrix} \begin{bmatrix} F_x(s) \\ F_y(s) \end{bmatrix} \quad (54)$$

Noting that

$$\begin{bmatrix} F_x(t) \\ F_y(t) \end{bmatrix} - \begin{bmatrix} F_x(t-T_t) \\ F_y(t-T_t) \end{bmatrix} = \begin{bmatrix} \Delta F_x(t) \\ \Delta F_y(t) \end{bmatrix} - \begin{bmatrix} \Delta F_x(t-T_t) \\ \Delta F_y(t-T_t) \end{bmatrix}$$

the structural displacements are related to the machining forces by

$$\begin{bmatrix} \Delta x(s) \\ \Delta y(s) \end{bmatrix} = (1 - e^{-sT_t}) [G_t(s) + G_p(s)] \begin{bmatrix} \Delta F_x(s) \\ \Delta F_y(s) \end{bmatrix} \quad (55)$$

Taking the Laplace transform of Eq. (52) with zero initial conditions, substituting the resulting equation into Eq. (55), and rearranging

$$\begin{bmatrix} \Delta F_x(s) \\ \Delta F_y(s) \end{bmatrix} \left[ I_2 - \frac{dN_t}{2\pi} (1 - e^{-sT_t}) G^0(s) \right] = \mathbf{0} \quad (56)$$

where  $I_2$  is the  $2 \times 2$  identity matrix and

$$G^0(s) = \frac{2\pi}{N_t} A^0 [G_t(s) + G_p(s)] \quad (57)$$

Equation (56) is now solved, based on the method presented by Budak and Altintas [5], to obtain the limiting depth-of-cut for stability. Assuming the steady-state solution is undamped and oscillates at a single chatter frequency  $\omega_c$ , Eq. (56) becomes

$$\begin{bmatrix} \Delta F_x(j\omega_c) \\ \Delta F_y(j\omega_c) \end{bmatrix} \left[ I_2 - \frac{dN_t}{2\pi} (1 - e^{-j\omega_c T_t}) G^0(j\omega_c) \right] = \mathbf{0} \quad (58)$$

For nontrivial solutions of Eq. (58)

$$\det \left[ I_2 - \frac{dN_t}{2\pi} (1 - e^{-j\omega_c T_t}) G^0(j\omega_c) \right] = \mathbf{0} \quad (59)$$

The parameter  $\Lambda$  is defined as

$$\Lambda = -\frac{dN_t}{2\pi} [1 - e^{-j\omega_c T_t}] = \Lambda_R + j\Lambda_I \quad (60)$$

Using the Euler identity and solving Eq. (60) for the limiting depth-of-cut

$$d = -\frac{\pi \Lambda_R}{N_t} (1 + \kappa^2) \quad (61)$$

where the parameter  $\kappa$  is given in Eq. (15), with  $T_t$  substituted for  $T$ . It should be noted that sometimes the thrust force is modeled as a fraction of the cutting force and that, in this case, the effect of the feed nonlinearity would be explicitly shown in Eq. (61) similar to the turning solution in Eq. (14). Using a similar procedure as in the previous section, the spindle speed corresponding to the limiting depth-of-cut given in Eq. (61) on the  $l$ th stability lobe is

$$N_s = \frac{60\omega_c}{N_t[\pi - 2\varphi + 2l\pi]} \quad l = 0, 1, 2, \dots \quad (62)$$

where  $\varepsilon = \pi - 2\varphi$  and  $\varphi = \tan^{-1}(\kappa)$ .

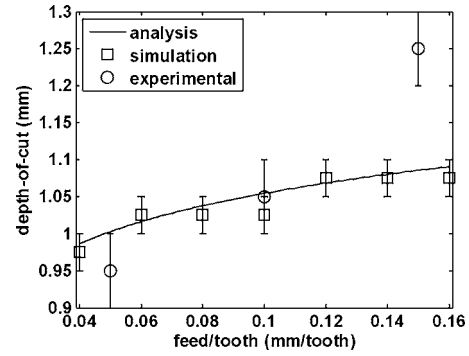


Fig. 5 Feed-depth stability lobe diagram for the face milling simulation—experimental study with  $N_s=1519$  rpm.

## Face Milling Simulation and Experimental Studies

Simulation and experimental studies are conducted in this section to investigate the effect that the force-feed nonlinearity has on chatter in face milling operations. The part is 6061 aluminum, the tool teeth are carbide with a lead angle of  $\psi_r=45$  deg, the tool radius is  $R_t=25$  mm, and the cutting fluid is air. Machining tests are conducted where the feed/tooth and depth-of-cut are varied between  $f_t=0.1-0.2$  mm/tooth and  $d=1-2$  mm, respectively, and the spindle speed is fixed at  $N_s=1519$  rpm. For the force process modeling tests, the tool has a single tooth,  $\theta_{en}=-27$  deg, and  $\theta_{ex}=27$  deg. The process parameters for the modeling tests were such that chatter was not present. The data are used to create the following cutting and thrust force models:  $F_C=1.25 \cdot d \cdot f^{0.933}$  and  $F_T=0.568 \cdot d \cdot f^{0.789}$ . The cutting tool and part structural models in both the  $x$  and  $y$  directions were created by conducting a series of impact and static deflection tests. It was determined that all four models are well characterized by a single mode and that the coupling was insignificant. The cutting tool and part transfer function matrices, respectively, are

$$G_t(s) = \begin{bmatrix} \frac{\omega_{xt}^2 k_{xt}^{-1}}{s^2 + 2\zeta_{xt}\omega_{xt}s + \omega_{xt}^2} & 0 \\ 0 & \frac{\omega_{yt}^2 k_{yt}^{-1}}{s^2 + 2\zeta_{yt}\omega_{yt}s + \omega_{yt}^2} \end{bmatrix} \quad (63)$$

$$G_p(s) = \begin{bmatrix} \frac{\omega_{xp}^2 k_{xp}^{-1}}{s^2 + 2\zeta_{xp}\omega_{xp}s + \omega_{xp}^2} & 0 \\ 0 & \frac{\omega_{yp}^2 k_{yp}^{-1}}{s^2 + 2\zeta_{yp}\omega_{yp}s + \omega_{yp}^2} \end{bmatrix} \quad (64)$$

where  $\omega_{xt}=4500$  rad/s,  $\omega_{yt}=4000$  rad/s,  $\omega_{xp}=2600$  rad/s,  $\omega_{yp}=2100$  rad/s,  $\zeta_{xt}=0.07$ ,  $\zeta_{yt}=0.11$ ,  $\zeta_{xp}=0.09$ ,  $\zeta_{yp}=0.22$ ,  $k_{xt}=k_{yt}=14$  kN/mm, and  $k_{xp}=k_{yp}=9.5$  kN/mm. See Landers [15] for a complete description of the force process and machine tool-part structure models, as well as the experimental procedures used to determine the model numerical parameters.

For the chatter simulation and experimental studies,  $\theta_{en}=-90$  deg,  $\theta_{ex}=90$  deg, and  $N_t=4$ . To determine a single TDS value, the closed-loop machining system is simulated with a fixed set of process parameters and the spectrum of  $F_z$  is examined. The depth-of-cut is then adjusted by 0.1 mm until marginal stability occurs. The experimental points are found in a similar manner. The results are shown in Fig. 5. The TDS and analysis correlates reasonably well with the experimental data. The differences can be attributed to the zeroth Fourier approximation of the force process matrix  $A$  and the granularity of the depth-of-cut adjustment. Again, since the nonlinear force-feed coefficients ( $\alpha_C=0.933$  and  $\alpha_T=0.789$ ) are less than one, the stability boundary increases for increasing feed in the feed range considered in this example.

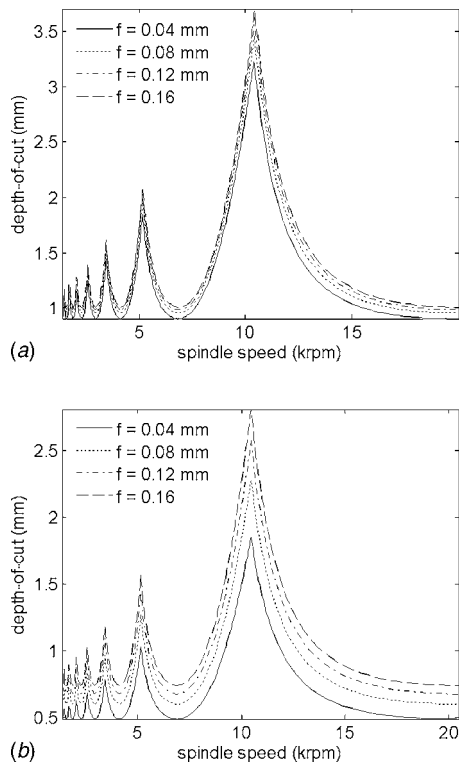


**Fig. 6 Stability lobe diagrams for the face milling simulation study with: (a)  $\alpha_C=0.933$  and  $\alpha_T=0.789$ ; and (b)  $\alpha_C=0.7$  and  $\alpha_T=0.7$**

However, the increase is very slight since the coefficients are close to unity. Complete stability lobe diagrams are also constructed for the first five lobes for feeds of 0.04 mm, 0.8 mm, 0.12 mm, and 0.16 mm. The results are shown in Fig. 6(a). It can be seen that as the feed increases, the limiting depth-of-cut increases. Again, the increase is very slight since the nonlinear force-feed coefficients are close to unity. The stability lobe diagrams were also constructed for the same system, except with  $\alpha_C=\alpha_T=0.7$ , and the results are shown in Fig. 6(b). Since the nonlinear force-feed coefficients are significantly less than unity, the nonlinear feed effect is more evident than in Fig. 6(a).

### Effect of Force-Feed Nonlinearity in End Milling Operations

In this section the effect that the force-feed nonlinearity has in end milling operations is investigated. To analyze chatter in end milling operations, the tool is decomposed into a series of slices along the axial direction. Each slice is modeled as a thin face mill with distinct entry and exit angles. The reader is referred to Budak and Altintas [5,16] for a complete chatter analysis of end milling operations. The nonlinear analysis of chatter in end milling operations is very similar to face milling operations and, for the sake of brevity, is omitted here. Instead, results are presented for a series of end milling experiments to explore the effect that the force-feed nonlinearity has on chatter in end milling operations.

For each experiment the part material is Ti6A4V, the end mill is solid carbide ( $N_f=8$ ,  $R_t=19.05$  mm), flood coolant is used, and  $d=19.05$  mm. Three spindle speeds, three widths-of-cut, and three feeds are utilized, for a combination of 27 experiments. The process parameters and coordinate system are shown in Fig. 7. Three orthogonal forces acting on the part are simultaneously measured using a Kistler 9752BA three component dynamometer. Chatter is determined by examining the force signals and their power spectral density plots. An example of one of the unstable end milling operations is shown in Fig. 8. In this experiment the spindle

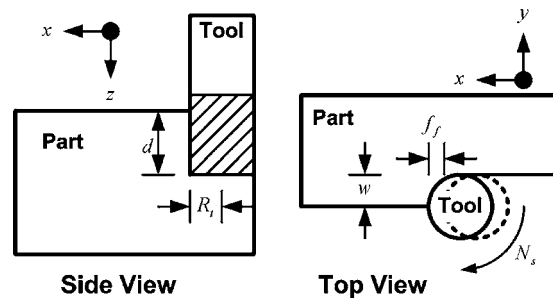


**Fig. 7 End milling operation schematics (dashed line is previous flute trajectory)**

speed, width-of-cut, and feed are 1750 rpm, 1.27 mm, and 0.0508 mm, respectively. High-frequency variations are evident in the force plots. The power spectral density plots show significant energy in all three force signals at 811 Hz. Since this frequency is not the tool rotation frequency, or a multiple of the tool rotation frequency, chatter was present in this operation. Note that the power spectral density plots also show significant energy at 29.2 Hz in the  $F_x$  signal, 116.7 Hz in the  $F_y$  signal, and 116.7 Hz and 233.5 Hz in the  $F_z$  signal. For a spindle speed of 1750 rpm, these frequencies are the tool rotation frequency (29.2 Hz) and four and eight multiplies (116.7 Hz and 233.5 Hz, respectively) of the tool rotation frequency. An example of one of the stable end milling operations is shown in Fig. 9. In this experiment the spindle speed, width-of-cut, and feed are 1750 rpm, 1.27 mm, and 0.1016 mm, respectively. For this case, there are no high-frequency variations in the force plots. The power spectral density plots show significant energy at 29.2 Hz and 233.5 Hz in the  $F_x$

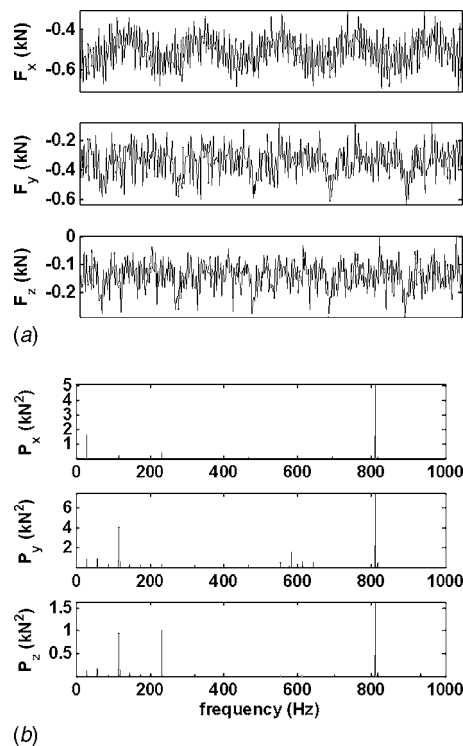


**Fig. 8 Experimental results for end milling of Ti6A4V with an eight-flute solid carbide end mill using flood coolant ( $N_s=1750$  rpm,  $f_f=0.0508$  mm,  $w=1.27$  mm,  $d=19.05$  mm). Machining forces for five spindle revolutions are given in the left plot and corresponding power spectral densities are given in the right plot.**

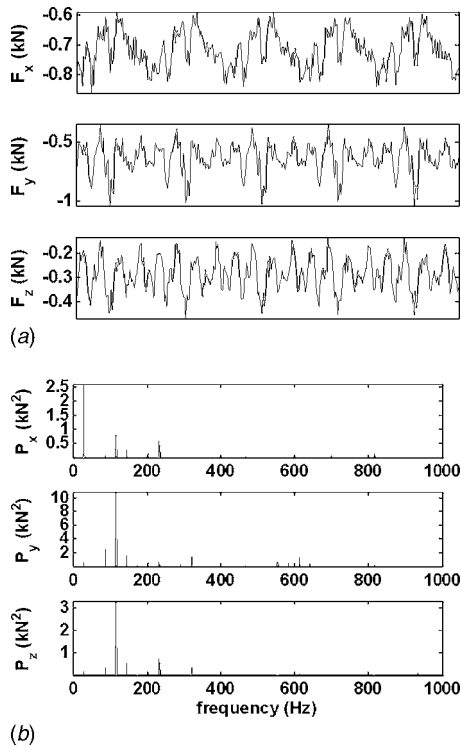


**Fig. 9** Experimental results for end milling of Ti6A4V with an eight-flute solid carbide end mill using flood coolant ( $N_s = 1750$  rpm,  $f_f = 0.1016$  mm,  $w = 1.27$  mm,  $d = 19.05$  mm). Machining forces for five spindle revolutions are given in the left plot and corresponding power spectral densities are given in the right plot.

signal, 116.7 Hz in the  $F_y$  signal, and 116.7 Hz and 233.5 Hz in the  $F_z$  signal. Since these are the tool rotation frequencies and multiples of the tool rotation frequency, the operation is stable.

The results for all 27 experiments are shown in Table 1. For a spindle speed of 1550 rpm and a width-of-cut of 1.27 mm, chatter was not present for all three values of feed and for a spindle speed/width-of-cut combinations of 1550 rpm/2.54 mm and 1750 rpm/2.54 mm, chatter was present for all three values of feed. However, for the other six combinations of spindle speeds and widths-of-cut, chatter was present for lower feeds, but not for higher feeds. The results demonstrate that the feed dramatically affects the presence of chatter and that, for this end milling operation, increasing the feed suppresses chatter. The results provide empirical evidence that the nonlinear thrust and cutting force-feed power coefficients are less than one.

**Table 1** Experimental results for end milling of Ti6A4V with an eight-flute solid carbide end mill using flood coolant ( $d = 19.05$  mm)

Spindle Speed (rpm)	Width of cut (mm)	Chatter (Yes/No)		
		$f = 0.0508$ (mm)	$f = 0.0762$ (mm)	$f = 0.1016$ (mm)
1350	1.27	Yes	No	No
1550	1.27	No	No	No
1750	1.27	Yes	No	No
1350	1.905	Yes	Yes	No
1550	1.905	Yes	Yes	No
1750	1.905	Yes	No	No
1350	2.54	Yes	Yes	No
1550	2.54	Yes	Yes	Yes
1750	2.54	Yes	Yes	Yes

## Summary and Conclusions

The linear chatter analysis technique developed by Budak and Altintas [5] was extended in this paper to account for the force-feed nonlinearity in both turning and face milling operations. The technique was compared to time domain simulations for both operations and to experimental results for a face milling operation. Also, experimental studies were conducted for end milling operations. The analyses and experimental results clearly demonstrate the effect that the force-feed nonlinearity, specifically the exponent  $\alpha$ , has on chatter in machining operations.

The analyses provide insight into the nonlinear force-feed effect. It was seen that the effective force process gain is a function of the nominal feed and that, for practical values of feed, the limiting depth-of-cut increases as feed increases if the exponent in the nonlinear relation is less than one, which is typical for common materials such as aluminums and steels. Increasing the feed allows the process engineer to simultaneously decrease cycle time while suppressing chatter. However, it should be noted that the machining forces will increase as the feed increases and other constraints (e.g., spindle power limitations, tooth chippage) may prevent feed from being used to suppress chatter. The analysis developed for turning operations compared very well to the time domain simulation results and the analysis developed for face milling operations compared very well to both the time domain simulation and experimental results. By directly including the force-feed nonlinearity in the chatter analysis, the need to calibrate the force process model at different feeds is alleviated. The force-feed nonlinear effect was also demonstrated for end milling operations where, for most of the combinations of spindle speed and width-of-cut, chatter was suppressed as the feed increased.

## Acknowledgment

The authors gratefully acknowledge the financial support of the National Science Foundation (Grant No. DDM-9313222), the University of Michigan's Engineering Research Center for Reconfigurable Machining Systems (NSF Grant No. EEC95-92125), and the Air Force Research Laboratory (Contract No. FA8650-04-C-5704).

## Nomenclature

- $A$  = linear force process matrix of directional coefficients
- $A^0$  = 0th-order Fourier approximation of  $A$
- $d$  = depth-of-cut (mm)
- $f$  = feed (mm)
- $f_f$  = feed/flute (mm/flute)
- $f_n$  = nominal feed (mm)
- $f_t$  = feed/tooth (mm/tooth)
- $F$  = longitudinal force (kN)
- $F_C$  = cutting force acting on tooth (kN)
- $F_{C_n}$  = nominal cutting force acting on tooth (kN)
- $F_n$  = nominal longitudinal force acting on tool (kN)
- $F_T$  = thrust force acting on tooth (kN)
- $F_{T_n}$  = nominal thrust force acting on tooth (kN)
- $F_x$  = force acting on tool in  $x$  direction (kN)
- $F_y$  = force acting on tool in  $y$  direction (kN)
- $F_z$  = force acting on tool in  $z$  direction (kN)
- $g$  = force-structure transfer function
- $G_t$  = force-machine tool structure transfer function matrix
- $G_p$  = force-part structure transfer function matrix
- $k$  = structural stiffness (kN/mm)
- $N_s$  = spindle speed (rpm)
- $N_f$  = number of flutes
- $N_t$  = number of tool teeth
- $P$  = longitudinal pressure (kN/mm<sup>2</sup>)
- $P_C$  = cutting pressure (kN/mm<sup>2</sup>)

$P_T$  = thrust pressure (kN/mm<sup>2</sup>)  
 $P_x$  = power spectral density of force acting on tool in  $x$  direction (kN<sup>2</sup>)  
 $P_y$  = power spectral density of force acting on tool in  $y$  direction (kN<sup>2</sup>)  
 $P_z$  = power spectral density of force acting on tool in  $z$  direction (kN<sup>2</sup>)  
 $R_t$  = tool radius (mm)  
 $s$  = Laplace variable  
 $t$  = time (s)  
 $T$  = spindle revolution period (s)  
 $T_t$  = tooth passing period (s)  
 $x_t$  = machine tool structural displacement in  $x$  direction (mm)  
 $x_p$  = part structural displacement in  $x$  direction (mm)  
 $y_t$  = machine tool structural displacement in  $y$  direction (mm)  
 $y_p$  = part structural displacement in  $y$  direction (mm)  
 $z$  = machine tool structural displacement in  $z$  direction (mm)  
 $\alpha$  = longitudinal force-feed power relationship exponent  
 $\alpha_C$  = cutting force-feed power relationship exponent  
 $\alpha_T$  = thrust force-feed power relationship exponent  
 $\sigma$  = function determining tooth-part contact  
 $\Delta F$  = longitudinal force acting on tool due to structural displacements (kN)  
 $\Delta F_x$  = force acting on tool in  $x$  direction due to structural displacements (kN)  
 $\Delta F_y$  = force acting on tool in  $y$  direction due to structural displacements (kN)  
 $\Delta x$  = difference between current and previous structural displacements in  $x$  direction (mm)  
 $\Delta y$  = difference between current and previous structural displacements in  $y$  direction (mm)  
 $\Delta z$  = difference between current and previous structural displacements in  $z$  direction (mm)  
 $\zeta$  = structural damping ratio  
 $\zeta_{xp}$  = part structural damping ratio in  $x$  direction  
 $\zeta_{xt}$  = machine tool structural damping ratio in  $x$  direction  
 $\zeta_{yp}$  = part structural damping ratio in  $y$  direction  
 $\zeta_{yt}$  = machine tool structural damping ratio in  $y$  direction  
 $\theta$  = angular tooth displacement (rad)  
 $\theta_{en}$  = entry angle (rad)  
 $\theta_{ex}$  = exit angle (rad)  
 $\psi_r$  = lead angle (rad)

$\omega_c$  = chatter frequency (rad/s)  
 $\omega_n$  = structural natural frequency (rad/s)  
 $\omega_{xp}$  = part structural natural frequency in  $x$  direction (rad/s)  
 $\omega_{xt}$  = machine tool structural natural frequency in  $x$  direction (rad/s)  
 $\omega_{yp}$  = part structural natural frequency in  $y$  direction (rad/s)  
 $\omega_{yt}$  = machine tool structural natural frequency in  $y$  direction (rad/s)

## References

- [1] Merritt, H. E., 1965, "Theory of Self-Excited Machine Tool Chatter: Contribution to Machine-Tool Chatter Research-1," *ASME J. Eng. Ind.*, **87**(4), pp. 447–454.
- [2] Sridhar, R., Hohn, R. E., and Lang, G. W., 1968, "A Stability Algorithm for the General Milling Process: Contribution to Machine Tool Chatter Research-7," *ASME J. Eng. Ind.*, **90**(2), pp. 330–334.
- [3] Minis, I., and Yanushevsky, R., 1993, "A New Theoretical Approach for the Prediction of Machine Tool Chatter in Milling," *ASME J. Eng. Ind.*, **115**(1), pp. 1–8.
- [4] Olgac, N., and Hosek, M., 1998, "A New Perspective and Analysis for Regenerative Machine Tool Chatter," *Int. J. Mach. Tools Manuf.*, **38**(7), pp. 783–798.
- [5] Budak, E., and Altintas, Y., 1998, "Analytical Prediction of Chatter Stability in Milling Part I: General Formulation," *ASME J. Dyn. Syst., Meas., Control*, **120**(1), pp. 22–30.
- [6] Landers, R. G., 2005, "Regenerative Chatter in Machine Tools," *Vibration and Shock Handbook*, C. W. DeSilva, ed., CRC Press, Boca Raton, FL, Chap. 35.
- [7] Jensen, S. A., and Shin, Y. C., 1999, "Stability Analysis in Face Milling Operations, Part 1: Theory of Stability Lobe Prediction," *ASME J. Manuf. Sci. Eng.*, **121**(4), pp. 600–605.
- [8] Jensen, S. A., and Shin, Y. C., 1999, "Stability Analysis in Face Milling Operations, Part 2: Experimental Validation and Influencing Factors," *ASME J. Manuf. Sci. Eng.*, **121**(4), pp. 606–614.
- [9] Tsai, M. D., Takata, S., Inui, M., Kimura, F., and Sata, T., 1990, "Prediction of Chatter Vibration by Means of a Model-Based Cutting Simulation System," *CIRP Ann.*, **39**(1), pp. 447–450.
- [10] Smith, S., and Tlustý, J., 1993, "Efficient Simulation Programs for Chatter in Milling," *CIRP Ann.*, **42**(1), pp. 463–466.
- [11] Weck, M., Altintas, Y., and Beer, C., 1994, "CAD Assisted Chatter-Free NC Tool Path Generation in Milling," *Int. J. Mach. Tools Manuf.*, **34**(6), pp. 879–891.
- [12] Zhang, H., and Ni, J., 1995, "Phase Difference and its Sensitivity Analysis for a Nonlinear Difference-Differential Machining Chatter Model," *Trans. NAMRI/SME*, **23**, pp. 131–136.
- [13] Endres, W. J., 1996, "The Effect of Uncut Chip Thickness Nonlinearity and Linear Process Gain Calculation on Machining Stability Analysis," *Proceedings ASME International Mechanical Engineering Conference and Exposition*, Atlanta, GA, Nov. 17–22, pp. 115–127.
- [14] Endres, W. J., 1996, "A Quantitative Energy-Based Method for Predicting Stability Limit as a Direct Function of Spindle Speed for High-Speed Machining," *Trans. NAMRI/SME*, **24**, pp. 27–32.
- [15] Landers, R. G., 1997, "Supervisory Machining Control," Ph.D. dissertation, University of Michigan, Ann Arbor, MI.
- [16] Budak, E., and Altintas, Y., 1998, "Analytical Prediction of Chatter Stability in Milling Part II: Application of the General Formulation to Common Milling Systems," *ASME J. Dyn. Syst., Meas., Control*, **120**(1), pp. 31–36.